Transition from symmetric to asymmetric local coercivity distribution in CoCrPt alloy films

Mi-Young Im,[1] Dong-Hyun Kim,[2] and Sung-Chul Shin[1]
[1]*Department of Physics and Center for Nanospinics of Spintronic Materials, Korea Advanced Institute of Science and Technology, Daejon 305-701, Korea*
[2]*Center for X-Ray Optics, Lawrence Berkeley National Laboratory, Berkeley, California 94720, USA*
(Received 21 August 2005; published 31 October 2005)

The local coercivity distribution of CoCrPt alloy films prepared by dc magnetron sputtering has been investigated by means of magneto-optical microscope magnetometer, capable of simultaneously measuring the local magnetic properties on a submicrometer spatial resolution. We find that with increasing Pt concentration the local coercivity distribution becomes asymmetric and the average local coercivity as well as the width of the distribution increases. Transmission electron microscopy studies, together with a theoretical explanation, reveal that the results are closely correlated with the grain size distribution dependent on the Pt concentration.

DOI: 10.1103/PhysRevB.72.132416 PACS number(s): 75.75.+a, 68.55.Jk, 75.70.Ak

CoCr-based alloy films are one of the most promising candidates for high-density perpendicular magnetic recording media because of their strong perpendicular magnetic anisotropy (PMA) and low media noise due to the decoupling of the exchange interaction between the magnetically isolated grains via the compositional segregation at grain boundaries.[1–6] In particular, CoCrPt alloy films have been extensively studied, since they provide desirable magnetic properties such as high coercivity and strong magnetocrystalline anisotropy for stable high-density recording.[7,8] In order to achieve high-density magnetic recording, it is essential to characterize the local magnetic property variation as well as the local microstructural property variation of films, since the local magnetic property variation that generally exists in real films due to the microstructural irregularity results in a crucial effect on magnetization reversal behavior and plays a decisive role in magnetic domain recording process.[9,10] So far, most previous studies on CoCrPt alloy films have been carried out to mainly investigate the microstructural properties such as grain size and grain size distribution. Intense efforts have also been done to control the grain size and the grain size distribution, which continues to be an important aspect of media processing and to suppress the media noise by reducing the intergranular exchange interaction between the neighboring grains.[11–16] However, no detailed study has been addressed on the submicrometer-scale local magnetic property variation in CoCrPt alloy films and also, the microscopic details of the correlation between the local magnetic property and the local microstructural property.

In this work, we report our systematic experimental investigations on the local magnetic property variation in CoCrPt alloy films with changing the Pt concentration and we clarify the origin of the local magnetic property variation. The local magnetic property variation has been observed by measuring the local coercivity distribution considering the fact that the coercivity is a structure-sensitive magnetic property. The local coercivity distribution is analyzed and discussed by comparing the microstructure of the film, together with a theoretical explanation based on a micromagnetic simulation considering the intergranular exchange interaction among grains.

Series of CoCrPt alloy films with varying Pt concentration were grown by dc magnetron cosputtering of CoCr alloy targets with Pt chips, where the Ti underlayer was first prepared onto a glass substrate to get better (002) hcp crystallographic alignment of CoCrPt alloy film. The Si_3N_4 layer of 500 Å was coated over the sample to induce a higher Kerr rotational angle. The film preparation conditions were optimized to obtain a film with PMA, where PMA was achieved for 400-Å $(Co_{82}Cr_{18})_{100-x}Pt_x$/1100-Å Ti alloy films under an Ar pressure of 3 mTorr at an ambient temperature, where $6 \leqslant x \leqslant 28$ at. %. The film growth orientation, film surface morphology, and the microstructure were characterized using a high-angle x-ray diffractometer, scanning electron microscope (SEM), and transmission electron microscope (TEM), respectively. The grain size and grain size distribution were estimated from the TEM image. The magnetic anisotropy constant and saturation magnetization of samples were measured by a torque magentometer and vibrating magnetometer, respectively.

The local coercivity distribution was investigated using a magneto-optical microscope magnetometer (MOMM). The MOMM system mainly consists of an optical polarizing microscope, capable of magnetic domain imaging by utilizing the magneto-optical Kerr effect. A charge coupled device (CCD) camera captures the domain image in the form of the array of the Kerr intensity measured from the CCD pixels with a spatial resolution of 400 nm. By storing the domain images and tracing the Kerr intensity variation for every individual CCD pixel sweeping the external magnetic field, it is possible to obtain an array of the local Kerr hysteresis loops. We want to stress that all the hysteresis loops of the local areas of a sample are simultaneously obtained from corresponding CCD pixels in each run. This enables us to avoid presumable measurement errors from different runs as well as the magnetic after effect due to a long measurement time.

We could generate the two-dimensional spatial distribution map of the local coercivity of the sample from directly analyzing the local hysteresis loops of every local area simultaneously measured with an identical condition of the sweeping rate of 10 Oe/s. A typical spatial distribution map of the local coercivity for the sample having Pt concentration of 6 at. % is demonstrated in Fig. 1. The local coercivity distribution was mapped by gray scale onto the two-dimensional *XY* plane, where each map corresponds to a

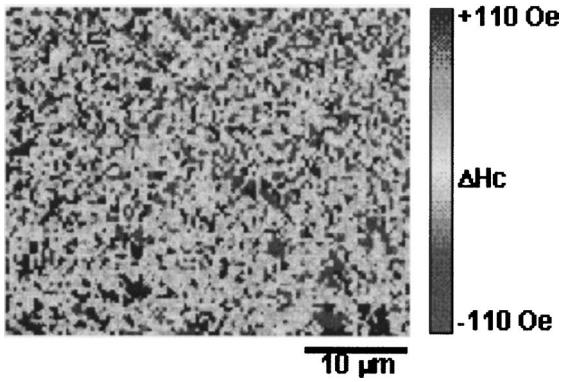

FIG. 1. Typical spatial local coercivity distribution map for 500-Å Si_3N_4/400-Å $(Co_{82}Cr_{18})_{94}Pt_6$/1100-Å Ti alloy film. The local coercivity distribution is mapped by gray scale in the two-dimensional *XY* plane, where each map corresponds to a sample surface area of 40×32 μm^2 and each pixel corresponds to an area of 400×400 nm^2.

sample surface area of 40×32 μm^2 and each pixel corresponds to an area of 400×400 nm^2, which is determined by the spatial resolution of our experimental setup. It can be considered that one pixel contains about 100 grains based on the microstructure observation by means of TEM. The shape of the local coercivity distribution was confirmed to be essentially the same in several repeated measurements. The figure clearly shows the spatial fluctuation of the local coercivity on a submicrometer scale. Note that the local coercivity distribution is completely random and no spatial correlation is observed among the neighboring local regions. The spatially random fluctuation of the local coercivity for CoCrPt alloy films is possibly ascribed to a weak exchange interaction due to grain isolation from compositional segregation at grain boundaries, which indeed has been reported in TEM studies for these films.[17] The typical surface morphology image of our sample is illustrated in Fig. 2, where the small isolated grains with the clear grain boundaries are observed. It is worthwhile to compare the present results with our previous ones for Co/Pd multilayer films,[18] which shows a smooth spatial variation of the local coercivity distribution due to the strong exchange interaction.

The local coercivity variation was also witnessed for the samples having different Pt concentrations. Interestingly

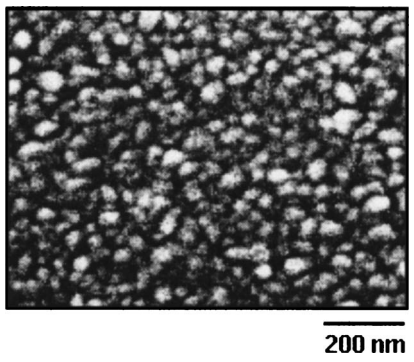

FIG. 2. Typical growth morphology image of 500-Å Si_3N_4/400-Å $(Co_{82}Cr_{18})_{94}Pt_6$/1100-Å Ti alloy film.

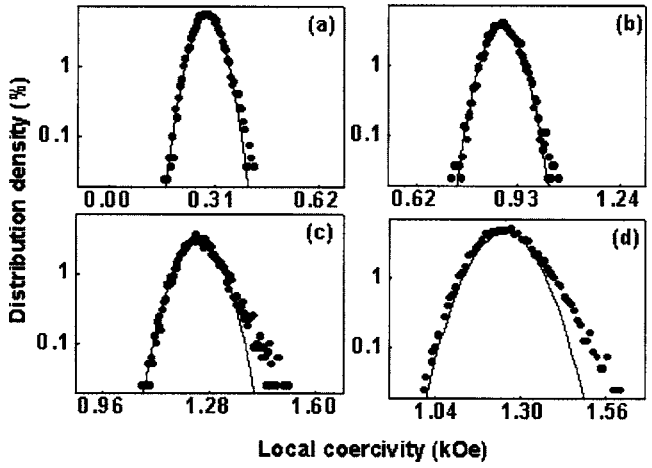

FIG. 3. Distribution density of the local coercivity of 500-Å Si_3N_4/400-Å $(Co_{82}Cr_{18})_{100-x}Pt_x$/1100-Å Ti alloy films with (a) $x=6$, (b) $x=13$, (c) $x=21$, and (d) $x=28$ at. %. The solid line is the best fit to the experimental data based on Gaussian distribution function.

enough, our experimental results reveal that the local coercivity distribution becomes asymmetric with increasing Pt concentration as demonstrated in Fig. 3. In the figure, we plot the local coercivity distribution density by counting the number of cells having the corresponding value of the local coercivity for every 10 Oe interval for the alloy films with Pt concentrations of (a) 6, (b) 13, (c) 21, and (d) 28 at. %. The distribution density is normalized by the total number of 8000 cells. It is clearly seen from the figure that the local coercivity distribution is getting more deviated from symmetric Gaussian distribution with increasing Pt concentration: the local coercivity distributions of the samples with $x=6$ at. % and 13 at. % show nearly symmetric, whereas the distributions of the samples with $x\geqslant21$ at. % are distinctively deviated from the symmetric distribution. It is also interesting to note that with increasing the Pt concentration from 6 to 28 at. % the average local coercivity and the full width half maximum (FWHM) of the local coercivity distribution monotonically increase from 0.43 to 1.3 kOe and from 0.17 to 0.34 kOe, respectively.

To understand the variation of the local coercivity distribution and the average local coercivity dependence on the Pt concentration, we have investigated the grain size and the grain size distribution in CoCrPt alloy films via an analysis of TEM images, considering the fact that they substantially influence the magnetic properties.[19] Grain size is defined as the diameter of a circle having the same projected area of the grain. In Fig. 4, we illustrate the grain size distributions of the samples with the Pt concentration of (a) 6, (b) 13, (c) 21, and (d) 28 at. %. As the Pt concentration varies from 6 to 28 at. %, the average grain size and the FWHM of the grain size are increased from 17 to 25 nm and from 7 to 12 nm, respectively. The grain size distributions of the samples with the Pt concentration of 6 at. % and 13 at. % are observed to be nearly symmetric, but one can clearly see asymmetric size distributions for the samples with the Pt concentration of 21 and 28 at. %.

Most interestingly, one can notice that with increasing Pt

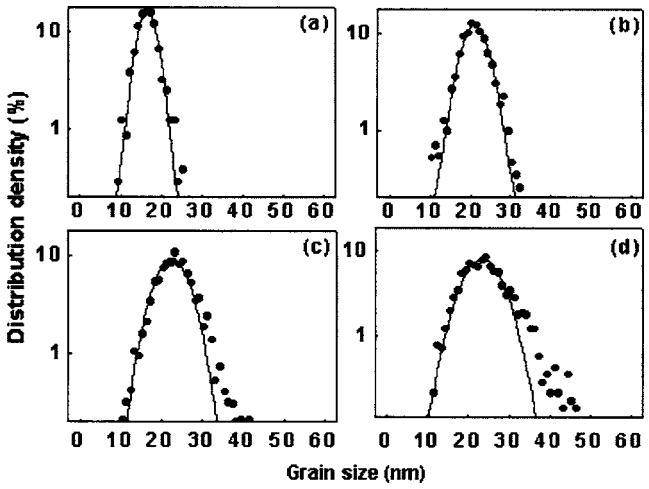

FIG. 4. Distribution density of the grain size of 500-Å Si_3N_4/400-Å $(Co_{82}Cr_{18})_{100-x}Pt_x$/1100-Å Ti alloy films with (a) $x=6$, (b) $x=13$, (c) $x=21$, and (d) $x=28$ at. %.

concentration the grain size distribution in Fig. 4 shows a similar trend that the distribution becomes broader and asymmetric as the local coercivity distribution in Fig. 3. These results strongly suggest the possibility of the direct correlation between the local coercivity distribution and the grain size distribution. To examine this possibility, we have to first consider an intergranular exchange interaction, since it is one of the important parameters in determination of the local coercivity distribution. The effect of intergranular exchange interaction on local coercivity has been investigated by performing the micromagnetic simulation using OOMMF.[20] The image obtained by image processing of the SEM image for the CoCrPt sample was used to generate the simulated system including grains and grain boundaries in OOMMF micromagnetic simulation. The processed image as exhibited in Fig. 5(a) consists of grains indexed by different gray levels and grain boundaries, which are defined as interfaces among grains. Micromagnetic simulation using OOMMF has been carried out with cell size of 10 nm in 400×400 nm^2 sample area, where this area is selected to be coincident with the CCD single pixel size in our experimental setup. The measured uniaxial magnetic anisotropy constant K_u of 5×10^6 erg/cc and the saturated magnetization M_s of 480 emu/cc were used as material parameters for the simulation. In our simulation, we assumed that intergranular exchange interaction among grains increased with Pt concentration, based on microstructural observations via TEM and SEM, which reveal the reduction of grain isolation and compositional segregation at grain boundaries with increasing Pt concentration. Actually, the increase of intergranular exchange interaction by the addition of Pt has been reported by previous studies of these systems.[4,12] The exchange constant (A_{ex}) among grains was changed from 1×10^{-12} J/m to 7×10^{-12} J/m with varying Pt concentration from 6 to 28 at. %, assuming that the exchange interaction among grains is proportional to the amount of Pt added, while A_{ex} within grains were kept at the same value of 1.5×10^{-11} J/m as that for pure Co, where smaller values of the exchange constants among grains are chosen over A_{ex} within grains, considering the decrement of exchange interaction among grains due to Cr segregation at grain boundaries. In Fig. 5(b), we demonstrate the simulated M-H hysteresis loops for the different exchange constant among grains of

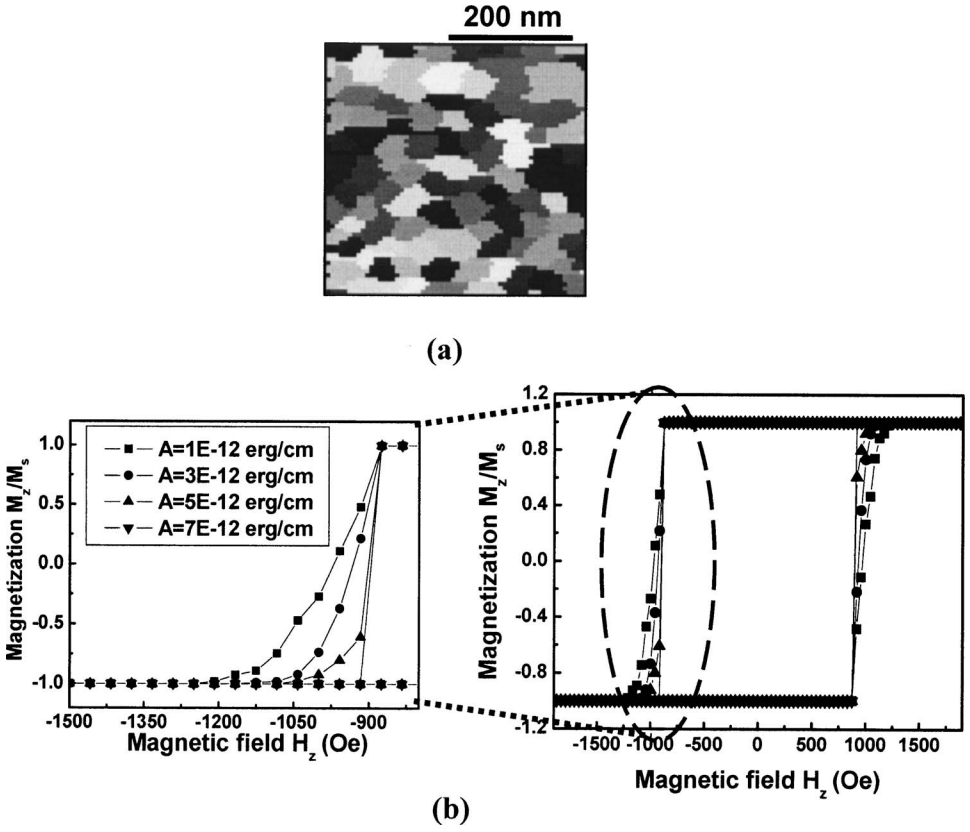

FIG. 5. (a) Image used for OOMMF micromagnetic simulation, here the different gray levels represent the different grains. (b) Micromagnetically simulated M-H hysteresis loops for the different exchange constant among grains of 1×10^{-12}, 3×10^{-12}, 5×10^{-12}, and 7×10^{-12} J/m.

1×10^{-12}, 3×10^{-12}, 5×10^{-12}, and 7×10^{-12} J/m, where one can notice that the coercivity of hysteresis loop is decreased by increasing the intergranular exchange constant dependent on Pt concentration. This result is contradictory to our result, which reveals the increase of average coercivity with Pt concentration (Fig. 3). In addition, it is expected that an exchange coupling among grains will give rise to more narrowed coercivity distribution due to a collective magnetization reversal of grain. Thus, one can conclude that the variation of the intergranular exchange interaction with Pt concentration does not play a dominant role in determining the variation of coercivity distribution in CoCrPt films.

Another important factor we should consider in our interpretation of the local coercivity distribution is the anisotropy constant (K_u) distribution in each grain. To investigate the role of K_u, we have measured the effective K_u for all samples using a torque magnetometer: it was revealed that K_u increased with increasing the Pt concentration. Measured values of K_u, coercivity, average grain size, and loop squareness with respect to the Pt concentration are illustrated in Fig. 6. Note that the overall trends of K_u, coercivity, and average grain size obtained in a macroscopic scale are quite similar to one another. The increase of squareness is considered to be originated from the increase of K_u, while the increase of K_u is ascribed to the improved crystallinity and enlarged grain size by adding Pt. If a grain is magnetically completely isolated and composed of a single magnetic domain, the coercivity of each grain will be proportional to the grain size. Indeed, our domain observation experiment by means of magnetic transmission x-ray microsopy proves that each grain is magnetically fully isolated and composed of a single domain.[21] Thus, one can conclude that the grain size distribution determines the coercivity distribution via K_u distribution in the grains. In this sense, it seems that the grain size distribution is the most dominant factor to influence the local coercivity and coercivity distribution and two distributions can be directly correlated, although they are on quite a different spatial scale.

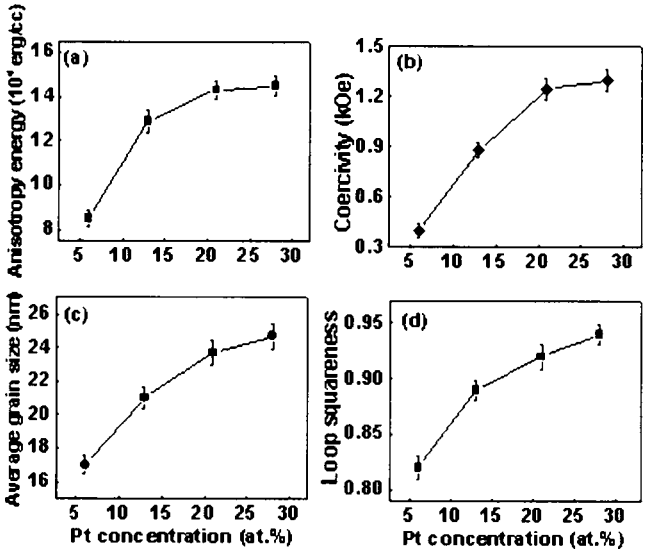

FIG. 6. (a) Effective anisotropy constant, (b) coercivity, (c) average grain size, and (d) loop squareness with respect to Pt concentration of 500-Å Si_3N_4/400-Å $(Co_{82}Cr_{18})_{100-x}Pt_x$/1100-Å Ti alloy films with $x=6$, 13, 21, and 28 at. %.

In conclusion, we have investigated the spatial distribution of the local coercivity on a submicrometer scale in CoCrPt alloy films by simultaneous local measurements, where the local coercivity distribution takes crossover from symmetric to asymmetric distribution with increasing the Pt concentration. The experimental result is understood by theoretical interpretation: the grain size distribution is a crucial effect on the local coercivity distribution in CoCrPt alloy films.

This work was supported (in part) by the Ministry of Science and Technology of Korea through the Cavendish-KAIST Research Cooperation Center. We thank H. G. Cho for assistance in measurement of TEM images, A. Perumal for helpful discussion.

[1] S. Iwasaki and Y. Nakamura, IEEE Trans. Magn. **13**, 1272 (1977).
[2] M. Sagoi and T. Inoue, J. Appl. Phys. **67**, 6394 (1990).
[3] N. Honda, S. Yanase, K. Ouchi, and S. Iwasaki, J. Appl. Phys. **85**, 6130 (1999).
[4] T. Keitoku, J. Ariake, N. Honda, K. Ouchi, and S. Iwasaki, J. Magn. Magn. Mater. **176**, 25 (1997).
[5] M. Futamoto, Y. Hirayama, N. Inaba, Y. Honda, K. Ito, A. Kikugawa, and T. Takeuchi, IEEE Trans. Magn. **35**, 2802 (1999).
[6] G. Wastlbauer, G. D. Skidmore, C. Merton, J. Schmidt, E. D. Dahlberg, and J. Skorjanec, Appl. Phys. Lett. **76**, 619 (2000).
[7] L. Tang, L. L. Lee, D. E. Laughlin, and D. N. Lambeth, Appl. Phys. Lett. **69**, 1163 (1996).
[8] O. Kitakami, N. Kikuchi, and S. Okamoto, J. Magn. Magn. Mater. **202**, 305 (1999).
[9] S.-B. Choe and S.-C. Shin, Phys. Rev. B **62**, 8646 (2000).
[10] S.-B. Choe and S.-C. Shin, Appl. Phys. Lett. **78**, 1430 (2001).
[11] Y. Matsuda, Y. Yahisa, J. Inagaki, and A. Ishikawa, J. Appl. Phys. **79**, 5351 (1996).
[12] N. Inaba, T. Yamamoto, Y. Hosoe, and M. Futamoto, J. Magn. Magn. Mater. **168**, 222 (1997).
[13] Y. Xu, J. P. Wang, and Y. Su, J. Appl. Phys. **87**, 6971 (2000).
[14] J. Zou, B. Lu, T. Leonhardt, D. E. Laughlin, and D. N. Lambeth, J. Appl. Phys. **87**, 6869 (2000).
[15] Y. Takahashi and Y. Yajima, J. Appl. Phys. **87**, 5699 (2000).
[16] S. Li and C. Potter, IEEE Trans. Magn. **37**, 1947 (2001).
[17] N. Inaba and M. Futamoto, J. Appl. Phys. **87**, 6863 (2000).
[18] S.-B. Choe and S.-C. Shin, Phys. Rev. B **65**, 224424 (2002).
[19] G. C. Hadjipanayis, J. Magn. Magn. Mater. **200**, 373 (1999).
[20] M. J. Donahue and D. G. Porter, OOMMF Users Guide Version 1.2a3.
[21] M. Y. Im, P. Fischer, T. Eimuller, G. Denbeaux, and S.-C. Shin, Appl. Phys. Lett. **83**, 4589 (2003).